

An Uncertainty Quantification Framework for Deep Learning-Based Automatic Modulation Classification

Huian Yang and Rajeev Sahay

Abstract—Deep learning has been shown to be highly effective for automatic modulation classification (AMC), which is a pivotal technology for next-generation cognitive communications. Yet, existing deep learning methods for AMC often lack robust mechanisms for uncertainty quantification (UQ). This limitation restricts their ability to produce accurate and reliable predictions in real-world environments, where signals can be perturbed as a result of several factors such as interference and low signal-to-noise ratios (SNR). To address this problem, we propose a deep ensemble approach that leverages multiple convolutional neural networks (CNNs) to generate predictive distributions, as opposed to point estimates produced by standard deep learning models, which produce statistical characteristics that quantify the uncertainty associated with each prediction. We validate our approach using real-world AMC data, evaluating performance through multiple UQ metrics in a variety of signal environments. Our results show that our proposed ensemble-based framework captures uncertainty to a greater degree compared to previously proposed baselines in multiple settings, including in-distribution samples, out-of-distribution samples, and low SNR signals. These findings highlight the strong UQ capabilities of our ensemble-based AMC approach, paving the way for more robust deep learning-based AMC.

Index Terms—Automatic modulation classification, deep ensembles, deep learning, out-of-distribution samples, uncertainty quantification,

I. INTRODUCTION

AUTOMATIC Modulation Classification (AMC) is a vital component of modern wireless networks, as it enables the identification of modulation schemes without prior knowledge of the transmitted signal. This capability is crucial for ensuring reliable communication in dynamic and noisy environments, including military [1], [2] and civilian applications [3], where signals can be subject to interference and environmental distortions. As the Internet of Things (IoT) expands, next-generation communications (e.g., 6G) will heavily rely on AMC for efficient management of the increasingly congested wireless spectrum [4], [5].

Traditional AMC methods, such as maximum likelihood-based (MLB) approaches [6]–[9], rely on statistical tests to estimate the probability of a particular modulation scheme. Although these methods can be effective, they require substantial prior knowledge about the received signal and its

channel conditions [10]. Furthermore, MLB methods tend to be computationally expensive, incurring high latencies while requiring manual feature engineering from received in-phase and quadrature (IQ) time samples. Such limitations restrict their scalability and adaptability into the high-volume IoT spectrum in real-world scenarios.

To address these challenges deep learning (DL) has recently emerged as a powerful alternative to MLB methods for AMC. DL models can efficiently learn distinguishing AMC characteristics from received IQ signals without requiring manual feature engineering while achieving state-of-the-art classification accuracy [3], [11]–[14]. As a result, they provide a promising alternative to MLB approaches to meet the demands of overcrowded next-generation cellular networks. However, despite their success, DL models exhibit a critical limitation. Specifically, deep learning-based AMC systems are frequently *overconfident* [15] in their predictions, even when they are incorrect, and often lack robust mechanisms for uncertainty quantification (UQ) to characterize the confidence associated with a given prediction. This overconfidence can result in significant performance degradations during deployment, particularly on incorrect predictions, when the model encounters previously unseen signal environments. Such overconfidence is further exacerbated in mission-critical settings, where decisions must be made under uncertainty, including low SNR conditions and adversarial scenarios [16], [17].

To address these challenges, we propose a UQ framework for AMC based on an ensemble of convolutional neural networks (CNNs), which generate predictive distributions, as opposed to point estimates produced by current state-of-the-art CNNs, whose statistical characteristics quantify the uncertainty associated with each prediction. Building on ensemble learning techniques [18]–[22], our approach provides calibrated uncertainty estimates, thereby enhancing reliability and robustness of current DL-based AMC frameworks. Compared to traditional UQ methods such as Bayesian Neural Networks (BNNs) [23], our proposed framework offers superior performance with lower computational overhead. Specifically, our method achieves higher classification accuracy in multiple signal environments, demonstrates better performance on out of distribution (OOD) samples such as adversarial examples [24]–[26]. Moreover, our ensemble-based approach is scalable to large-parameter architectures such as ResNet [27], enabling existing DL-based AMC frameworks to improve their performance while simultaneously incorporating UQ for

H. Yang and R. Sahay are with the Department of Electrical and Computer Engineering, UC San Diego, San Diego, CA, 92093 USA. E-mail: {huy011,r2sahay}@ucsd.edu.

This work was supported in part by the UC San Diego Academic Senate under grant RG114404.

increased robustness.

Our specific contributions of this work can be summarized as follows:

- 1) **Deep Ensemble Framework for AMC:** We develop a robust ensemble-based AMC framework comprised of multiple CNNs. *To the best of our knowledge, this is the first ensemble-based deep learning UQ framework for AMC.*
- 2) **UQ Characterization in AMC:** For the first time, we develop UQ metrics that characterize the uncertainty associated with each received signal's modulation prediction. In comparison to other considered baselines, under a range of UQ metrics, we show that our method demonstrates significantly higher robustness by consistently scoring higher on these metrics.
- 3) **Out of Distribution Testing:** We test our framework on OOD samples, via adversarial perturbations, and show improved resistance to these perturbations, highlighting its UQ capability on shifted signal distributions.

The remainder of this paper is organized as follows. Sec. II reviews related work on DL-based AMC including uncertainty estimation in AMC, the robustness of ensemble learning, and recent expansions of UQ in AMC. Sec. III outlines our methodology, detailing the signal modeling process, ensemble modeling, estimation metrics, and the characterization of OOD samples. Sec. IV describes our experimental setup, presents UQ scoring and estimation results, and evaluates OOD performance. Finally, we close with concluding thoughts and future directions in Sec. V.

II. RELATED WORKS

Earlier methods for AMC relied on likelihood methods [7], [9], [10], which provided theoretical guarantees as well as uncertainty estimation. However, such methods incur computational inefficiency in large-scale networks, making them difficult to adopt in the increasingly congested wireless spectrum. DL, as an alternative to MLB approaches, has gained significant attention for AMC due to its state-of-the-art classification performance and significantly lower inference latencies compared to MLB approaches. In this regard, various neural network architectures have been explored such as CNNs [3], [4], [28], [29], recurrent neural networks (RNNs) [30]–[32], and long short-term memory (LSTM) [33]. By learning hierarchical features directly from raw signals, these DL approaches, in addition to having low online latencies, often excel in AMC classification tasks with little to no need for feature engineering. However, while prior studies have demonstrated the efficiency of DL compared to MLB approaches for AMC, less attention has been given to the UQ capabilities of these methods, which is the focus of our work.

More recently, Bayesian neural networks (BNNs) [34] have been proposed to perform DL-based AMC with UQ capabilities. Although BNNs seemingly provide the advantage of both the high classification performance of DL as well as UQ capabilities, their practical application is hindered by lower classification performance compared to state-of-the-art CNNs. Despite their ability to capture predictive distribution and

variance, which aids in uncertainty estimation, BNNs often have significantly lower classification performance compared to CNNs for AMC. This gap in performance and adaptability motivates our development of ensemble-based UQ methods for AMC.

Ensemble learning has emerged as a compelling alternative to BNNs in multiple domains, such as image processing [19] and bioinformatics [35], where multiple models are jointly analyzed. Compared to single models, deep ensembles yield superior classification performance [36] and generate predictive distributions instead of point estimates, leading to well-calibrated UQ estimates [19], [21], [37]. Additionally, deep ensembles have demonstrated higher classification accuracy in the presence of data distortions such as OOD samples, which have been shown to limit the efficacy of DL-based AMC methods [24]–[26].

Despite these successes in various other domains, the use of ensemble learning for UQ in AMC, or for signal processing tasks in general, remains unexplored. In this work, we leverage ensemble-based methods to demonstrate their effectiveness in quantifying uncertainty in AMC. Our framework not only achieves robust performance across a range of modulation types but is also scalable to state-of-the-art DL models, highlighting its adaptability in existing DL-based AMC frameworks.

III. METHODOLOGY

In this section, we develop our deep ensemble-based AMC framework and describe the metrics used to quantify the uncertainty of each model. We begin by discussing our AMC signal model in Sec. III-A. We then present our deep ensemble approach in Sec. III-B. Subsequently, Sec. III-C details the estimation metrics employed to evaluate the performance of different methods. Finally, Sec. III-D discusses our approach for analyzing OOD AMC signals.

A. Signal Modeling

In our considered wireless communication environment, a transmitter transmits $\mathbf{s} = [s[0], \dots, s[\ell-1]]$ through a channel $\mathbf{h} \in \mathbb{C}^\ell$, where $\mathbf{h} = [h[0], \dots, h[\ell-1]]^T$ captures radio imperfections and selective fading and ℓ denotes the length of the received signal's observation window. We model the received signal as

$$\mathbf{r} = \sqrt{\rho}\mathbf{H}\mathbf{s} + \mathbf{n}, \quad (1)$$

where $\mathbf{H} = \text{diag}\{h[0], \dots, h[\ell-1]\} \in \mathbb{C}^{\ell \times \ell}$, $\mathbf{n} \in \mathbb{C}^\ell$ represents additive white Gaussian noise (AWGN), and ρ denotes the signal to noise ratio (SNR), which is typically unknown at receiver further motivating the need for a UQ-based AMC framework. Moreover, we map each received baseband signal to a two-dimensional real matrix, $\mathbf{r} \in \mathbb{C}^\ell \rightarrow \mathbf{r} \in \mathbb{R}^{\ell \times 2}$ where the first and second column of \mathbf{r} represent the in-phase and quadrature components, respectively, of \mathbf{r} for compatibility with real-valued neural networks.

The receiver aims to perform AMC by calculating $\text{argmax}_i P(m_i|\mathbf{r}, \theta)$, where θ parameterizes the model used to calculate the AMC probability (further discussed in Sec. III-B), $m_i \in \mathcal{M}$, and $\mathcal{M} = \{m_1, \dots, m_C\}$ represents the set of considered modulation constellations. We assume that

the receiver uses $\mathcal{X}_{\text{tr}} = \{\mathbf{r}(n), \mathbf{y}(n); n = 1, \dots, N\}$ and $\mathcal{X}_{\text{te}} = \{\mathbf{r}(t), \mathbf{y}(t); t = 1, \dots, T\}$ as the training and testing datasets, respectively, where $\mathcal{X}_{\text{tr}} \cap \mathcal{X}_{\text{te}} = \emptyset$.

B. Ensemble Modeling

Data-driven AMC models, alone, cannot effectively characterize the uncertainty associated with their predictions because they tend to produce overconfident outputs. To address this limitation, we adopt an ensemble modeling approach consisting of multiple state-of-the-art deep learning AMC classifiers [38]. Unlike a standalone model, ensemble predictions cannot be obtained directly because multiple models are used simultaneously. To ensure diversity in predictions, each classifier is initialized with random parameters while maintaining the same architecture, resulting in each model converging to different local minima thus ensuring parallelized training as well as diverse predictions despite training on the same dataset [18]. As a result, the ensemble exhibits variability, yielding varying levels of confidence on samples that are known to be difficult for deep learning classifiers to operate on such as low SNR signals. As a result, analyzing the joint output prediction from each classifier in the ensemble simultaneously improves the UQ of the model.

We denote our ensemble as $\theta = \{\theta_b\}_{b=1}^B$ where B denotes the number of classifiers in the ensemble and θ_b parameterizes the b^{th} model. Each AMC classifier in the ensemble is a deep learning model with a softmax output. We denote each deep learning classifier as $f_{\theta_b}(\mathbf{r}) : \mathbb{R}^{\ell \times 2} \rightarrow \mathbb{R}^C$, parameterized by θ_b . Here, the b^{th} model aims to map the received signal $\mathbf{r} \in \mathbb{R}^{\ell \times 2}$ to a modulation constellation $\mathbf{y} \in \mathbb{R}^C$, where $C = |\mathcal{M}|$ represents the total number of possible modulation constellations. Due to the softmax classifier, $f_{\theta_b}(\mathbf{r})$ outputs $\hat{\mathbf{y}}^{(b)} \in \mathbb{R}^C$, where $\hat{y}_i^{(b)} = P(m_i | \mathbf{r}, \theta^{(b)}) \in \mathbb{R}$ (i.e., $\hat{y}_i^{(b)}$ is the i^{th} element of $\hat{\mathbf{y}}^{(b)}$ and denotes the probability assigned by the b^{th} classifier that the input \mathbf{r} is modulated according to constellation m_i). We train each AMC classifier in the ensemble by optimizing

$$\min_{\theta_b} \mathcal{L}(\theta_b, \mathbf{r}, \mathbf{y}), \quad (2)$$

where

$$\mathcal{L}(\theta_b, \mathbf{r}, \mathbf{y}) = -\frac{1}{N} \sum_{i=1}^N \sum_{j=1}^C \mathbf{y}_{ij} \log(\hat{y}_{ij}), \quad (3)$$

$\mathbf{y}_{ij} \in \mathbb{R}$ is j^{th} element of $\mathbf{y} \in \mathbb{R}^C$ corresponding to the i^{th} signal, and $\hat{y}_{ij} \in \mathbb{R}$ is j^{th} element of $\hat{\mathbf{y}} \in \mathbb{R}^C$, the predicted label, corresponding to the i^{th} signal.

During evaluation, we jointly analyze the prediction from all B classifiers in the ensemble to obtain

$$P(m_i | \mathbf{r}, \theta) = \frac{1}{B} \sum_{b=1}^B P(m_i | \mathbf{r}, \theta^{(b)}), \quad (4)$$

where $\text{argmax}_i P(m_i | \mathbf{r}, \theta)$ yields the predicted modulation constellation from the ensemble. In addition to obtaining the probability with which the input belongs to a particular modulation classification, we use the distributive estimate produced by the ensemble to characterize additional UQ metrics, which are discussed in Sec. III-C.

C. Estimation Metrics

Beyond obtaining the modulation classification estimate given in (4), we also employ several proper UQ scoring metrics [19] to assess model performance comprehensively. In this capacity, we consider the negative log-likelihood (NLL), the Brier score, the width of the prediction's confidence interval (CI), the coverage of the prediction, and set of high-confidence predictions.

The NLL quantifies the likelihood of the predicted probabilities aligning with the true labels and is given over the entire testing set by

$$-\frac{1}{T} \sum_{t=1}^T \sum_{j=1}^C \mathbf{y}_{tj} \log(\hat{y}_{tj}), \quad (5)$$

where lower NLL values indicate that the model assigns higher confidence to the correct classes, reflecting better alignment between predictions and true labels. Similarly, the Brier score, which measures the mean squared difference between the predicted probabilities and the actual outcomes, is computed over all samples and classes and is given by

$$\frac{1}{T} \sum_{t=1}^T \sum_{j=1}^C (\mathbf{y}_{tj} - \hat{y}_{tj})^2, \quad (6)$$

where lower Brier score values indicate that the model's probabilistic predictions are closer to ground truth values, minimizing deviations.

In addition, we also analyze the Confidence Interval (CI) widths, which characterize the ensemble's uncertainty in each prediction. A higher CI width indicates higher uncertainty, as the models comprising the ensemble vary to a higher degree in their predictions, whereas lower CI widths indicate lower uncertainty as the majority of models agree about the predicted modulation class. Ideally, we aim for a wide range of CI widths rather than a concentration within a narrow range, as seen with singular deep learning models, which indicates overconfidence. The upper and lower bounds of the CI of the t^{th} sample belonging to the j^{th} constellation are given by

$$\hat{y}_{tj} \pm z_{\alpha} \cdot \sqrt{\frac{S^2}{B}}, \quad (7)$$

z_{α} is the $1 - \alpha/2$ quantile of a zero-mean unit variance Gaussian distribution, and S^2 is the variance of the predicted probability among models, and the CI width is given by the computing the difference between the upper and lower bounds of (7).

We next calculate the coverage proportion, which evaluates the number of samples in the testing set whose true label is within the z_{α} CI. In computing the coverage of the ensemble, we consider two scenarios. First, we employ a strict condition, where the CI of the true class must contain one and the CI of all other classes must contain zero. This scenario strictly requires the ensemble to be certain that the predicted sample simultaneously (i) is modulated according to the predicted class and (ii) is not modulated according to any other class. Second, we relax these conditions and only require the CI of the true class to contain one and we do not consider the CIs

of the other classes. This metric, in both scenarios, quantifies the proportion of samples that the ensemble is expected to be confident in. This scenario is particularly helpful for low SNR signals, which often suffer from lower classification performance in data-driven AMC approaches.

Lastly, we define the high confidence set to evaluate the frequency with which the ensemble is highly confident in its predictions. A high confidence prediction occurs when $\operatorname{argmax}_i P(m_i | \mathbf{r}, \theta) > 0.8$. A high confidence prediction indicates overconfidence, which often occurs in singular deep learning models, while a low confidence prediction reflects under-confidence. Ideally, the ensemble should strike a balance, avoiding both extremes.

D. Out-of-distribution Samples

To further assess the robustness of our framework and simulate real-world environmental factors, we generate adversarial examples, denoted as \mathbf{r}' , which are considered OOD samples [39]. Deep learning AMC classifiers are highly susceptible to adversarial examples as they induce erroneous predictions, reflected in the softmax output of standalone models, particularly on high SNR signals. Although approaches to mitigate such samples have been investigated [40]–[42], they specifically target improving the robustness to adversarial attacks and do not consider the general UQ capabilities of the model. These samples degrade classification performance by pushing the received signal across the decision boundaries of DL models. This phenomenon is often represented as an adversarial perturbation, $\delta \in \mathbb{R}^{\ell \times 2}$, which is introduced to existing samples and formulated as

$$\begin{aligned} & \min_{\delta} \|\delta\|_{\infty} \\ \text{s.t. } & f_{\theta_b}(\mathbf{r}) \neq f_{\theta_b}(\mathbf{r} + \delta) \\ & \mathbf{r} + \delta \in \mathbb{R}^{\ell \times 2} \end{aligned} \quad (8)$$

where $\mathbf{r}' = \mathbf{r} + \delta$ represents the perturbed version of \mathbf{r} and $\|\cdot\|_{\infty}$ denotes the ℓ_{∞} norm bound of δ . Note that adversarial attacks using other norm bounds (e.g., the l_0 , l_1 , or l_2 bound) can also be generated, but we select the l_{∞} bound as it perturbs each sample thus helping in shift the sample away from its true distribution, which is our overall objective.

In practice it is difficult to analytically solve (8) due to its excessive non-linearity. Thus, solution to (8) are approximated in practice. In this work, we utilize the Fast Gradient Sign Method (FGSM) [43], to approximate a solution to (8), which is given by

$$\mathbf{r}' = \mathbf{r} + \epsilon \operatorname{sign}(\nabla_{\mathbf{r}} \mathcal{L}(\theta_b, \mathbf{r}, \mathbf{y})), \quad (9)$$

where $\epsilon = \|\delta\|_{\infty}$ represents the l_{∞} -bounded perturbation magnitude applied to the input samples.

We quantify the effect of the additive perturbation using the perturbation-to-noise ratio (PNR) [24]. Here, we compute the expected value of the power of the perturbation $\mathbb{E}[\|\delta\|_2^2]$ and then obtain the expected value of the power of the received signal $\mathbb{E}[\|\mathbf{r}\|_2^2]$. Using these quantities, along with the SNR of the received signal, the PNR is given by

$$\text{PNR [dB]} = \frac{\mathbb{E}[\|\delta\|_2^2]}{\mathbb{E}[\|\mathbf{r}\|_2^2]} [\text{dB}] + \text{SNR [dB]}, \quad (10)$$

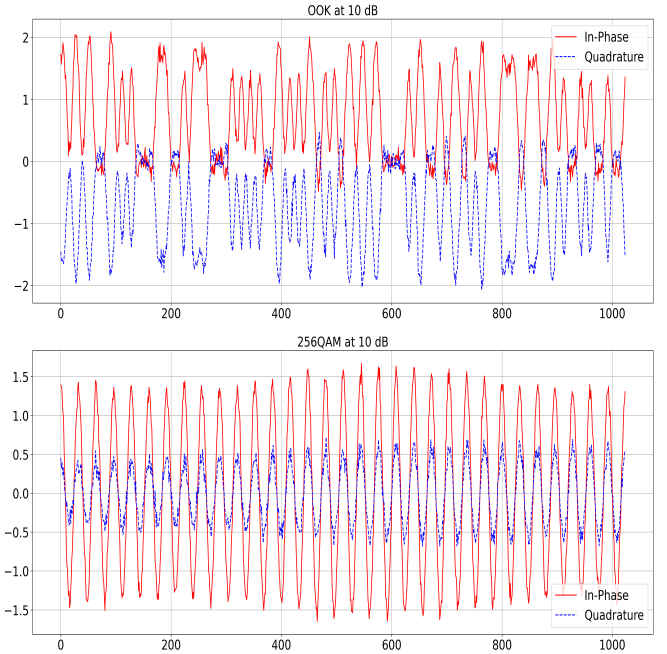


Fig. 1: Sample modulation constellations used for AMC in our empirical evaluations including OOK (top) and 256QAM (bottom) from the RML 2018.01a dataset.

where a lower PNR indicates that the perturbation is less potent and has a smaller effect on the distribution shift of \mathbf{r} whereas a higher PNR shift \mathbf{r}' further from \mathbf{r} and is more likely to satisfy the constraints of (8).

IV. PERFORMANCE EVALUATION

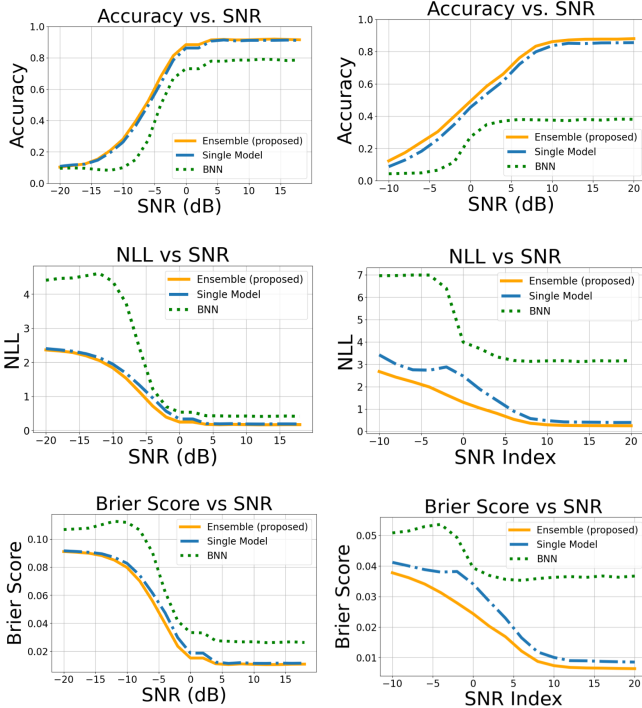
In this section, we assess the effectiveness of our proposed UQ framework for AMC. We begin by detailing our experimental setup in Sec. IV-A. In Sec. IV-B, we provide an in-depth analysis of the uncertainty estimation capabilities of our proposed framework compared to the proposed baselines. Finally, in Sec. IV-C, we investigate our framework’s robustness to out-of-distribution (OOD) samples and adversarial perturbations, a critical consideration for deploying AMC systems in real-world, dynamic environments.

A. Experimental Setup

We perform our empirical evaluation on two AMC datasets: RadioML2016.10a [44] and RadioML2018.01a [11]. RadioML2016.10a is a synthetic dataset generated using GNU radio while RadioML2018.01a is collected over-the-air on a wireless testbed making it a more difficult dataset but a better representation of real-world AMC data. RadioML2016.10a is comprised of $C = 11$ modulation types ranging from -10 dB to 20 dB SNR in increments of 2 dB. For each SNR, the dataset contains $12,000$ signals, where $\ell = 128$ samples in length. In comparison, RadioML2018.01a is an over-the-air dataset that contains $C = 24$ modulation types, ranging from -20 dB to 18 dB in increments of 2 dB, with each signal consisting of $\ell = 1024$ samples and consists of $19,661$ signals per SNR. Fig. 1 visualizes selected constellations used in our analysis. In each experiment, we use and $80\%/20\%$ split of the signals

TABLE I: The CNN architecture of each classifier in our ensemble.

Layer	Dropout Rate (%)	Activation	Shape
Conv 1	20	ReLU	$3 \times 1 \times 256$
Conv 2	20	ReLU	$3 \times 2 \times 128$
Conv 3	20	ReLU	$3 \times 1 \times 64$
Conv 4	20	ReLU	$3 \times 1 \times 64$
Flatten	-	-	-
Dense	-	ReLU	128
Output	-	Softmax	24

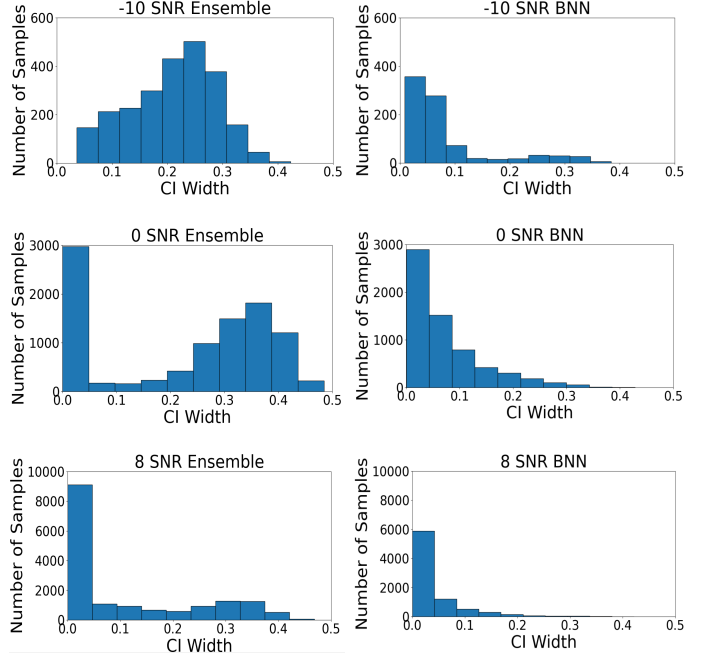
**Fig. 2:** UQ metrics on the 2016.10a (left column) and RML 2018.01a (right column) datasets. We see that our proposed ensemble model outperforms both considered baselines on each considered metric for both datasets.

at each SNR to form \mathcal{X}_{tr} and \mathcal{X}_{te} . \mathcal{X}_{tr} is used to train each classifier in the ensemble. After training, we report the UQ characteristics of the ensemble on \mathcal{X}_{te} .

Our framework employs an ensemble of $B = 15$ CNNs, selected for their demonstrated effectiveness in AMC tasks [29]. All models share the same architecture, which is shown in Table I and are all independently trained on \mathcal{X}_{tr} by minimizing (3) using stochastic gradient descent (SGD). Each model in the ensemble is trained using 100 epochs, a batch size of 256, and a learning rate of 0.001. Although we use the CNN architecture shown in Table I, our framework can be extended to incorporate an ensemble of classifiers with any architecture. As we will show, our ensemble of AMC classifiers consistently outperforms a standalone AMC classifier with the same architecture.

B. Uncertainty Quantification

In this section, we examine our framework’s UQ capabilities across a range of SNRs. In addition, we compare the performance of our framework to the two most common

**Fig. 3:** Correctly predicted CI widths of our proposed ensemble (left column) and the baseline BNN approach (right column) on RML 2018.01a. Here, we see that our ensemble has wider CI widths compared to the BNN, demonstrating that our proposed ensemble approach can characterize uncertainty to a higher extent in comparison to the BNN.

approaches for data-driven AMC with UQ: a standalone CNN classifier [7], [9], [10] and an AMC-based BNN [34]. The CNN is a single deep learning classifier that provides state-of-the-art performance but limited UQ capabilities. BNNs are another deep learning-based AMC framework capable of quantifying uncertainty better than standalone deep learning models by generating predictive distributions over point estimates, similar to our proposed ensemble, during inference. Yet, as we will show in our empirical analysis, BNNs suffer in baseline classification performance in comparison to state-of-the-art standalone deep learning classifiers. Contrary to both of these methods, we will see that our proposed deep ensemble framework for AMC provides both state-of-the-art classification performance as well as robust UQ.

Fig. 2 shows the performance of our approach in comparison to each considered baselines in terms of our considered scoring metrics. As shown in Fig. 2, our ensemble-based approach consistently outperforms both a standalone CNN and a BNN across the two datasets. Notably, while the single CNN and the ensemble exhibit relatively stable accuracy in both datasets, the BNN’s accuracy declines sharply on the RML 2018.01a dataset – likely due to the more complex real-world signals in it compared to the GNU radio generated data in the RML 2016.10a dataset —highlighting its limitations in AMC applications. Despite these challenges, the ensemble maintains the highest overall accuracy. Similarly, Fig. 2 shows that our proposed also outperforms the standalone CNN and the BNN, in terms of NLL, consistently achieving a lower NLL score across the entire SNR range. The BNN, in particular, consis-

tently attains a high NLL, relative to our proposed ensemble, in both considered datasets at each considered SNR. Lastly, we see from Fig. 2 that our ensemble consistently achieves the lowest Brier scores in all considered environments, further demonstrating its robustness relative to the other considered baselines.

In Fig. 3, we show the CI widths of low, medium, and high SNR values of our proposed ensemble model in comparison to BNNs on correctly predicted signals. In this scenario, we omit results from the standalone CNN, as they produce point predictions, resulting in CI widths of zero. From Fig. 3, we observe that, at -10 dB (low SNR), the BNN exhibits a mix of narrow and moderate CI widths, suggesting some level of uncertainty in low-SNR conditions. However, as the SNR increases to 0 dB and 8 dB, the BNN’s CI widths shift toward smaller values, indicating greater confidence in its predictions. This behavior aligns with expectations, as higher SNR leads to cleaner input data, reducing uncertainty. In contrast, our proposed ensemble model maintains a higher degree of uncertainty across all SNR levels, with wider CI widths than the BNN. However, as SNR increases, the ensemble also becomes more confident in its correct predictions, while still preserving some uncertainty in certain cases. Notably, our proposed ensemble achieves higher classification accuracy than the BNN (as shown in Fig. 2), despite its broader confidence intervals. This suggests that while the ensemble model expresses more uncertainty, it does not come at the cost of accuracy. Instead, it offers a more calibrated representation of confidence, ensuring that even in high-SNR conditions, some uncertainty is retained where appropriate.

We now turn our focus to the CI widths of low, medium, and high SNR values of our proposed ensemble model, in comparison to BNNs, on incorrectly predicted signals. In this scenario, robust uncertainty is demonstrated with high CI widths as we would not want a model to express high confidence in a wrong AMC prediction. As shown in Fig. 4, at -10 dB, the BNN primarily produces near-zero CI widths, meaning it is overconfident even when it is wrong. This misplaced confidence persists at higher SNRs (e.g., 0 dB and 8 dB), indicating that the BNN fails to appropriately capture uncertainty in its misclassifications. In contrast, our proposed ensemble exhibits wider CI widths for incorrect predictions, suggesting that it remains more cautious, especially in low-SNR environments, where the performance of deep learning-based AMC classifiers is known to struggle. As the SNR increases, our proposed ensemble’s average CI width remains wide, reflecting an appropriate level of uncertainty even in moderate to low noise conditions. Meanwhile, the BNN’s overconfidence remains evident across all SNR levels, failing to distinguish between correct and incorrect predictions in terms of uncertainty representation.

Next, we assess coverage proportions in Fig. 5, which describe how well each model’s predictive intervals capture the true class. A higher coverage indicates stronger uncertainty representation. Here, we omit the coverage of the single model since it produces point estimates, which results in coverage proportions 0. In Fig. 5, we see that the ensemble outperforms both considered baselines, particularly surpassing the coverage

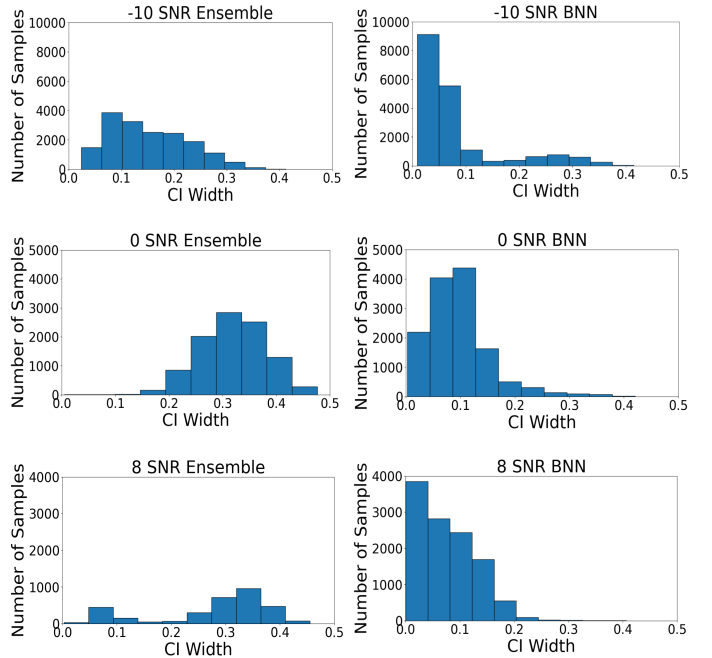


Fig. 4: Incorrectly predicted CI widths of our proposed ensemble (left column) and the baseline BNN approach (right column) on RML 2018.01a. Similar to Fig. 3, we see here that our ensemble produces wider CI widths compared to the BNN, demonstrating that our proposed ensemble can more effectively characterize uncertainty estimates, particularly on incorrectly predicted signals.

proportions of BNNs. Moreover, we see this trend hold for both the strict and relaxed definitions of coverage (as defined in Sec. III-B), indicating that our proposed ensemble can represent, to a higher degree than the BNN, both its uncertainty associated with its predicted class as well its uncertainty associated with its prediction that the input does not belong to any other class.

Lastly, we evaluate high-confidence sets in Fig. 6, where we label a prediction as high-confidence if the model assigns at least an 80% probability to a particular class (as elaborated on in Sec. III-B). The standalone CNN leads in this category, reflecting its tendency to be overconfident. Conversely, the BNN struggles with underconfidence, consistently producing fewer high-confidence predictions. Our proposed ensemble model strikes a balanced approach, achieving strong accuracy while also retaining suitable uncertainty, even at higher SNR levels for its high-confidence prediction, reinforcing its ability to characterize uncertainty to a higher degree in comparison to the considered baselines.

C. Out-of-Distribution Performance

Here, we examine how our framework handles OOD scenarios by examining its effects on adversarial examples. Although they are typically below the noise floor of wireless signals, adversarial perturbations can significantly degrade the performance of neural network-based AMC methods by inducing models to output incorrect predictions due to their underlying shifted distributions [45].

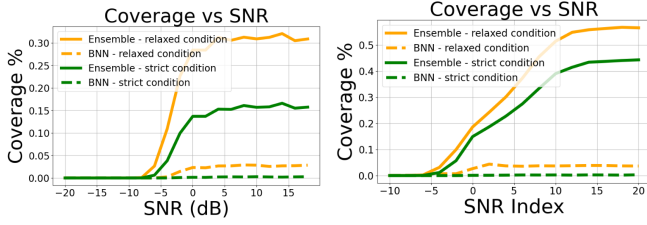


Fig. 5: Coverage proportion, under strict and relaxed conditions, of our approach in comparison to each considered baseline. Here, we see that our proposed ensemble achieves a higher coverage proportion under both the strict and relaxed conditions for RML 2016.10a (left) and RML 2018.01a (right). This indicates that our proposed ensemble excels in its predictive interval, ensuring that the true class is more likely to be contained.

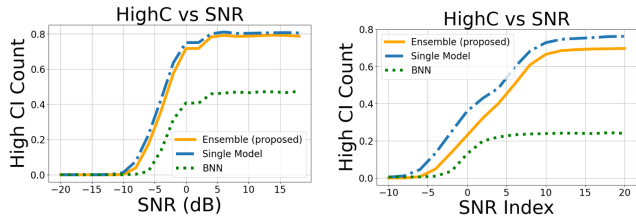


Fig. 6: High confidence proportion of our proposed ensemble in comparison to each considered baseline. In both RML 2016.10a (left) and RML 2018.01a (right), our ensemble maintains a middle level between the CNN and BNN, indicating that the ensemble is neither overconfident nor underconfident compared to the other models.

We first examine the effect of adding a constant PNR of 5 dB across the entire SNR range. Fig. 7 displays each model’s accuracy on unperturbed samples for comparison. While the ensemble and the standalone CNN show similar performance on clean signals, the ensemble significantly outperforms the CNN on OOD AMC signals. This disparity highlights the ensemble’s superior UQ capabilities in challenging signal environments. We next examine our proposed ensemble’s accuracy across increasing PNRs at a constant SNR of 10 dB. As the PNR increases, the perturbed sample is shifted further from its unperturbed counterpart, thereby increasing the chance of misclassification and further shifting the distribution of the adversarial examples. Fig. 8 includes accuracies under normal (unperturbed) conditions, shown as straight lines since SNR remains constant. Here, we see that even as the PNR increases, our proposed ensemble is able to withstand the performance degradation to a greater extent than both the CNN and the BNN. Overall, these findings highlight our proposed ensemble’s ability to retain robust performance under adversarial attacks, reinforcing its ability to characterize UQ to a greater extent in comparison to the considered baselines while simultaneously striking a balance between high confidence and well-calibrated uncertainty.

V. CONCLUSION

Deep Learning (DL) has been shown to provide cutting-edge performance in automatic modification classification (AMC). However, DL-based AMC models often exhibit overconfidence in their predictions, with no associated measure of

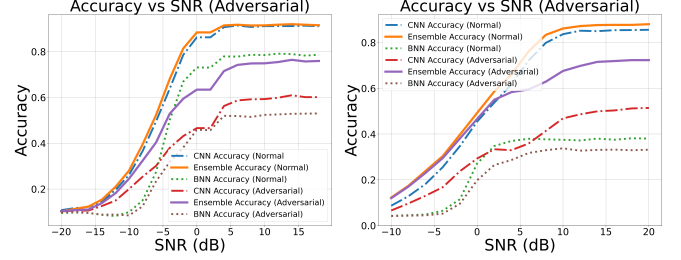


Fig. 7: Accuracy after applying a constant perturbation of 5 dB across varying SNRs on 2016.10a (left) and 2018.01a (right). The results demonstrate that, under both normal and adversarial conditions, our ensemble model achieves the best performance at high and low SNR values.

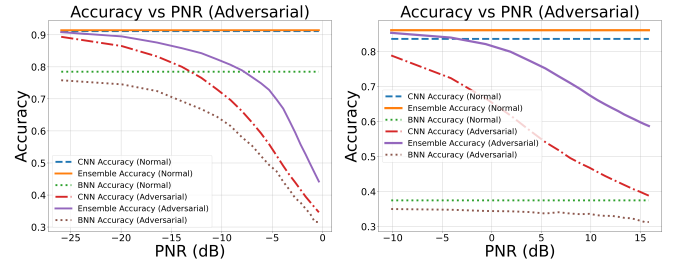


Fig. 8: Accuracy after varying the perturbation on 10 dB SNR signals on the 2016.10a (left) and 2018.01a (right) dataset. Here, we see that our proposed ensemble is able to maintain higher performance in comparison to the considered baselines as the PNR increases and approaches the noise floor.

uncertainty. This issue is especially evident in low signal to noise ratio (SNR) conditions and when handling out-of-distribution (OOD) samples. In this work, we proposed a deep ensemble framework for AMC, which is capable of retaining the state-of-the-art performance of DL-based AMC classifiers while simultaneously providing robust uncertainty quantification (UQ) metrics. We demonstrated our ensemble’s ability to achieve robust performance across multiple UQ metrics such as the negative log-likelihood, Brier score, prediction interval widths, prediction coverage, and high-confidence predictions. In comparison to standalone CNNs as well as Bayesian Neural Networks (BNNs), we showed that our framework achieved better UQ estimates overall, particularly in low SNR and OOD environments. Moreover, our proposed framework is scalable to any DL architecture, allowing state-of-the-art performance to be extended to incorporate higher classification performance as well as uncertainty quantification on any DL-based AMC framework. Future work will explore the resilience of our approach in more versatile environments such as the distributed AMC scenario, which requires UQ in federated learning with varying channel conditions and adversarial interference at each receiver, and in environments with insufficient channel state information (CSI) knowledge.

REFERENCES

- [1] G. Vanhoy, N. Thurston, A. Burger, J. Breckenridge, and T. Bose, “Hierarchical modulation classification using deep learning,” in *IEEE Military Communications Conference (MILCOM)*, 2018, pp. 20–25.

- [2] W. H. Clark, V. Arndorfer, B. Tamir, D. Kim, C. Vives, H. Morris, L. Wong, and W. C. Headley, "Developing rfml intuition: An automatic modulation classification architecture case study," in *IEEE Military Communications Conference (MILCOM)*, 2019, pp. 292–298.
- [3] G. J. Mendis, J. Wei, and A. Madanayake, "Deep learning-based automated modulation classification for cognitive radio," in *IEEE International Conference on Communication Systems (ICCS)*, 2016, pp. 1–6.
- [4] O. Kaya, M. A. Karabulut, A. F. M. S. Shah, and H. Ilhan, "Modulation classifier based on deep learning for beyond 5g communications," in *47th International Conference on Telecommunications and Signal Processing (TSP)*, 2024, pp. 336–339.
- [5] T. Huynh-The, Q.-V. Pham, T.-V. Nguyen, T. T. Nguyen, R. Ruby, M. Zeng, and D.-S. Kim, "Automatic modulation classification: A deep architecture survey," *IEEE Access*, vol. 9, pp. 142 950–142 971, 2021.
- [6] J. L. Xu, W. Su, and M. Zhou, "Likelihood-ratio approaches to automatic modulation classification," *IEEE Transactions on Systems, Man, and Cybernetics*, vol. 41, no. 4, pp. 455–469, 2011.
- [7] A. O. Abdul Salam, R. E. Sheriff, S. R. Al-Araji, K. Mezher, and Q. Nasir, "A unified practical approach to modulation classification in cognitive radio using likelihood-based techniques," in *IEEE 28th Canadian Conference on Electrical and Computer Engineering (CCECE)*, 2015, pp. 1024–1029.
- [8] M. Abu-Romoh, A. Aboutaleb, and Z. Rezki, "Automatic modulation classification using moments and likelihood maximization," *IEEE Communications Letters*, vol. 22, no. 5, pp. 938–941, 2018.
- [9] W. Wei and J. Mendel, "Maximum-likelihood classification for digital amplitude-phase modulations," *IEEE Transactions on Communications*, vol. 48, no. 2, pp. 189–193, 2000.
- [10] F. Hameed, O. A. Dobre, and D. C. Popescu, "On the likelihood-based approach to modulation classification," *IEEE Transactions on Wireless Communications*, vol. 8, no. 12, pp. 5884–5892, 2009.
- [11] T. J. O'Shea, T. Roy, and T. C. Clancy, "Over-the-air deep learning based radio signal classification," *IEEE Journal of Selected Topics in Signal Processing*, vol. 12, no. 1, pp. 168–179, 2018.
- [12] T. T. An and B. M. Lee, "Robust automatic modulation classification in low signal to noise ratio," *IEEE Access*, vol. 11, pp. 7860–7872, 2023.
- [13] Y. Wang, J. Yang, M. Liu, and G. Gui, "Lightamc: Lightweight automatic modulation classification via deep learning and compressive sensing," *IEEE Transactions on Vehicular Technology*, vol. 69, no. 3, pp. 3491–3495, 2020.
- [14] X. Fu, G. Gui, Y. Wang, H. Gacanin, and F. Adachi, "Automatic modulation classification based on decentralized learning and ensemble learning," *IEEE Transactions on Vehicular Technology*, vol. 71, no. 7, pp. 7942–7946, 2022.
- [15] J. Moon, J. Kim, Y. Shin, and S. Hwang, "Confidence-aware learning for deep neural networks," in *37th International Conference on Machine Learning*. PMLR, 13–18 Jul 2020, pp. 7034–7044.
- [16] R. Sahay, D. J. Love, and C. G. Brinton, "Robust automatic modulation classification in the presence of adversarial attacks," in *55th IEEE Annual Conference on Information Sciences and Systems (CISS)*, 2021, pp. 1–6.
- [17] J. Bai, C. Ge, Z. Xiao, H. Jiang, T. Li, H. Zhou, and L. Jiao, "A multiscale discriminative attack method for automatic modulation classification," *IEEE Transactions on Information Forensics and Security*, vol. 20, pp. 294–308, 2025.
- [18] R. Rahaman and A. H. Thiery, "Uncertainty quantification and deep ensembles," *Advances in neural information processing systems*, vol. 34, pp. 20 063–20 075, 2021.
- [19] B. Lakshminarayanan, A. Pritzel, and C. Blundell, "Simple and scalable predictive uncertainty estimation using deep ensembles," *Advances in neural information processing systems*, vol. 30, 2017.
- [20] R. Sahay, D. Ries, J. D. Zollweg, and C. G. Brinton, "Hyperspectral image target detection using deep ensembles for robust uncertainty quantification," in *55th IEEE Asilomar Conference on Signals, Systems, and Computers*, 2021, pp. 1715–1719.
- [21] N. Shi, F. Lai, R. Al Kontar, and M. Chowdhury, "Fed-ensemble: Ensemble models in federated learning for improved generalization and uncertainty quantification," *IEEE Transactions on Automation Science and Engineering*, vol. 21, no. 3, pp. 2792–2803, 2024.
- [22] G. Franchi, A. Bursuc, E. Aldea, S. Dubuisson, and I. Bloch, "One versus all for deep neural network for uncertainty (ovnni) quantification," *IEEE Access*, vol. 10, pp. 7300–7312, 2022.
- [23] F. Fiedler and S. Lucia, "Improved uncertainty quantification for neural networks with bayesian last layer," *IEEE Access*, vol. 11, pp. 123 149–123 160, 2023.
- [24] M. Sadeghi and E. G. Larsson, "Adversarial attacks on deep-learning based radio signal classification," *IEEE Wireless Communications Letters*, vol. 8, no. 1, pp. 213–216, 2019.
- [25] B. Flowers, R. M. Buehrer, and W. C. Headley, "Evaluating adversarial evasion attacks in the context of wireless communications," *IEEE Transactions on Information Forensics and Security*, vol. 15, pp. 1102–1113, 2020.
- [26] X. Yuan, P. He, Q. Zhu, and X. Li, "Adversarial examples: Attacks and defenses for deep learning," *IEEE Transactions on Neural Networks and Learning Systems*, vol. 30, no. 9, pp. 2805–2824, 2019.
- [27] K. He, X. Zhang, S. Ren, and J. Sun, "Deep residual learning for image recognition," in *2016 IEEE Conference on Computer Vision and Pattern Recognition (CVPR)*, 2016, pp. 770–778.
- [28] F. Meng, P. Chen, L. Wu, and X. Wang, "Automatic modulation classification: A deep learning enabled approach," *IEEE Transactions on Vehicular Technology*, vol. 67, no. 11, pp. 10 760–10 772, 2018.
- [29] A. P. Hermawan, R. R. Ginanjar, D.-S. Kim, and J.-M. Lee, "Cnn-based automatic modulation classification for beyond 5g communications," *IEEE Communications Letters*, vol. 24, no. 5, pp. 1038–1041, 2020.
- [30] S. Huang, R. Dai, J. Huang, Y. Yao, Y. Gao, F. Ning, and Z. Feng, "Automatic modulation classification using gated recurrent residual network," *IEEE Internet of Things Journal*, vol. 7, no. 8, pp. 7795–7807, 2020.
- [31] D. Hong, Z. Zhang, and X. Xu, "Automatic modulation classification using recurrent neural networks," in *3rd IEEE International Conference on Computer and Communications (ICCC)*, 2017, pp. 695–700.
- [32] S. Hu, Y. Pei, P. P. Liang, and Y.-C. Liang, "Deep neural network for robust modulation classification under uncertain noise conditions," *IEEE Transactions on Vehicular Technology*, vol. 69, no. 1, pp. 564–577, 2020.
- [33] S. Raghunandan and S. Begaj, "Analysis of deep neural networks for automatic modulation classification," in *40th International Communications Satellite Systems Conference (ICSSC 2023)*, 2023, pp. 117–122.
- [34] V.-C. Luu, J. Park, and J.-P. Hong, "Uncertainty-aware incremental automatic modulation classification with bayesian neural network," *IEEE Internet of Things Journal*, vol. 11, no. 13, pp. 24 300–24 309, 2024.
- [35] Y. Cao, T. A. Geddes, J. Y. H. Yang, and P. Yang, "Ensemble deep learning in bioinformatics," *Nature Machine Intelligence*, vol. 2, no. 9, pp. 500–508, 2020.
- [36] S. Ali, S. S. Tirumala, and A. Sarrafzadeh, "Ensemble learning methods for decision making: Status and future prospects," in *International Conference on Machine Learning and Cybernetics (ICMLC)*, vol. 1, 2015, pp. 211–216.
- [37] R. Sahay, J. J. Stubbs, C. G. Brinton, and G. C. Birch, "An uncertainty quantification framework for counter unmanned aircraft systems using deep ensembles," *IEEE Sensors Journal*, vol. 22, no. 21, pp. 20 896–20 909, 2022.
- [38] R. R. Yakkati, R. R. Yakkati, R. K. Tripathy, and L. R. Cenkeramaddi, "Radio frequency spectrum sensing by automatic modulation classification in cognitive radio system using multiscale deep cnn," *IEEE Sensors Journal*, vol. 22, no. 1, pp. 926–938, 2022.
- [39] N. Karunanayake, R. Gunawardena, S. Seneviratne, and S. Chawla, "Out-of-distribution data: An acquaintance of adversarial examples—a survey," *arXiv preprint arXiv:2404.05219*, 2024.
- [40] R. Sahay, C. G. Brinton, and D. J. Love, "A deep ensemble-based wireless receiver architecture for mitigating adversarial attacks in automatic modulation classification," *IEEE Transactions on Cognitive Communications and Networking*, vol. 8, no. 1, pp. 71–85, 2022.
- [41] R. Sahay, D. J. Love, and C. G. Brinton, "Robust automatic modulation classification in the presence of adversarial attacks," in *55th Annual Conference on Information Sciences and Systems (CISS)*, 2021, pp. 1–6.
- [42] P. Qi, T. Jiang, L. Wang, X. Yuan, and Z. Li, "Detection tolerant black-box adversarial attack against automatic modulation classification with deep learning," *IEEE Transactions on Reliability*, vol. 71, no. 2, pp. 674–686, 2022.
- [43] I. J. Goodfellow, J. Shlens, and C. Szegedy, "Explaining and harnessing adversarial examples," *arXiv preprint arXiv:1412.6572*, 2014.
- [44] T. O'Shea and N. West, "Radio machine learning dataset generation with gnu radio," *Proceedings of the GNU Radio Conference*, vol. 1, no. 1, 2016.
- [45] P. Qi, T. Jiang, L. Wang, X. Yuan, and Z. Li, "Detection tolerant black-box adversarial attack against automatic modulation classification with deep learning," *IEEE Transactions on Reliability*, vol. 71, no. 2, pp. 674–686, 2022.